Enhancement of Visible Light Backscatter Communication by Optimally Locating the Tags

Wentao Lin and Deepak Mishra
School of Electrical Engineering and Telecommunications, University of New South Wales, Sydney, NSW 2052, Australia
Emails: wentao.lin@student.unsw.edu.au and d.mishra@unsw.edu.au

***Abstract*—The visible light backscatter communication system has the advantages of sniffing and biological friendliness over the conventional radio frequency (RF) range one, which is essential in indoor communication. In this paper, we focus on the global optimally locating the tag to maximize the effective signal-noise ratio (SNR) in both the single-tag and the two-tags models. Closed-form expressions for the global-optimal locations of the tag are obtained for both two models by using the proposed novel expression of the effective SNR which includes consideration of physical blocking by tags and the optimization of time allocated to each tag for backscattering. Numerical results show that in one tag model, the optimized location of the tag should be placed close to the transmitter. In the two-tags model, one tag should be placed close to the transmitter and another should be placed close to the receiver. Lastly, it is noted that more than 5dB enhancement in effective SNR can be achieved by optimally locating the tags.**

I. Introduction

Backscatter communication is a hot technology to achieve the internet of thing (IoT) vision [1]. Visible light backscatter communication (VLC backscattering) has advantages on power efficiency [2], and it can use low-cost photo-diodes (PD) as a receiver without complex processing [3]. The location of tag is a important issue in the VLC backscattering, so this paper focused on optimizing the location of tags to maximize the effective signal to noise ratio (SNR).

A. Literature Review

Some prior studies showed that the network capacity of VLC backscattering can be increased by optimizing the reflection coefficient of tags [4]. The performance of SNR and interference between tags were studied in [5] and it gave the insight of optimizing both the location of tag and transmitter in each travel path, but it is a work for multiple tags and transmitters which contains more than ten tags and transmitters. The amount of energy harvested and reflected by the tag from the transmitter is the main index to determine a successful backscatter communication [6], [7]. The relationship among the communication distance, SNR, and bit error rate (BER) was indicated in [8] and [9]. They also indicated that deploying multiple-pixelated tags in VLC backscattering can increase the power harvested by the tag and overcome the single-channel power gain limitation. The SNR of VLC backscattering was improved by considering multiple-input multiple-output (MIMO) spatial diversity of tags in [9].

B. Motivation and Contribution

VLC backscatter communication provides long-range, less interference, and more precise indoor communication [10]. The highly directional property facilitates a favorable sniffing function that correctly aligns the VLC system-guided optics with more precise positioning capabilities. At the same time, it also has no interference with ambient RF and electromagnetic waves which is an essential advantage in indoor communication [1], [2]. However, the optimization of tags has not been considered. We would like to address this gap because as noted from the literature on optimal relay placement [11], by optimally locating the tags, the corresponding VLC backscatter communication performance can be significantly enhanced. This paper fits that gap and our main contribution is four-fold. (1) Considering the single-tag VLC backscattering model, we show that the effective SNR at the receiver is a concave function of the location of the tag. Closed-form expressions of the optimal location were derived. (2) The novel expression of the sum of effective SNR is obtained under the practical constraint of blocking in the two tags model. (3) Joint concavity of this effective SNR in the two-tags model in terms of locations of two tags and effective transmitting time of each tag is proved. Closed-form expressions for the optimal location are also derived. (4) Numerical results have been provided to gain insights into tags' locations for different values of system parameters and showing achievable gains due to it.

II. System Model

A. Adopted Topology for VLC Backscattering

In this paper, we consider both single-tag model and two-tags model. The single-tag model of VLC backscattering comprises a transmitter, a tag and a receiver as shown in Fig. 1(a) below, whereas the four nodes topology comprises of one transmitter, two tags and one receiver as shown in Fig. 1(b) below. The locations of transmitter and receiver are fixed. Each tag is combined with an LCD shutter and a retroreflector.

B. Channel Model for VLC Backscattering

1) Single-Tag Model: In Fig. 1(a), the distance between transmitter and receiver is labeled as D, and the distance between tag and receiver is labeled as d. Here m is the Lambertian order with $m = -\frac{\ln 2}{\ln(\cos\varphi_{1/2})}$ where $\varphi_{1/2}$ is the half power angle [12]. The channel power gain between transmitter and tag is donated as h_1 and the channel power

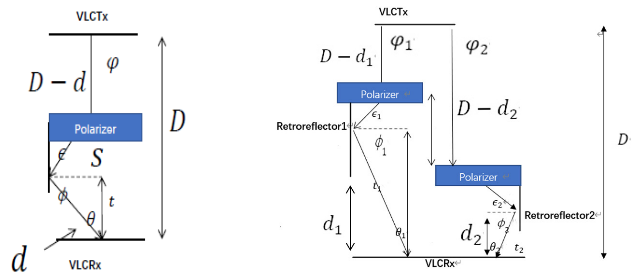

(a) Single tag model (b) Two tags model

Fig. 1: (a). The one tag model, (b). two tags model

gain between tag and receiver is defined as h_2. They are given by [13]:

$$h_1 = \frac{A_{tag}(m+1)g_x}{2\pi(D-d)^2}\cos^m\varphi\cos\epsilon, \tag{1}$$

$$h_2 = \frac{A_{PD}g_x}{2\pi d^2}\cos\phi\cos\theta, \tag{2}$$

In the Fig. 1(a), the φ is the angle of the irradiance respect to the transmitter vertically, θ is the incidence angle of the receiver, ϵ is the incidence angle of the tag, and ϕ is the irradiance angle of the tag [14], [15]. The g_x is modulation index where $g_x < 1$. A_{tag} is the cross area of the square tag and and A_{PD} is the cross area of receiver.

2) Two-Tags Model: The channel power gains from transmitter to each tag at two-tags model are h_{d1} and h_{d2} [13].

$$h_{di} = \frac{A_{tagi}(m+1)g_x}{2\pi(D-d_i)^2}\cos^m\varphi_i\cos\epsilon_i, \forall i = 1,2 \tag{3}$$

where φ_i is the angles of the irradiance respect to the transmitter vertically, θ_i is the incidence angles of the receiver, ϵ_i is the incidence angle of the tags, ϕ_i is the irradiance angle of the tags for all i=1,2 [14], [15].

From Fig. 1(a), s is the horizontal distance from tag to receiver (Rx). The distance from tag to Rx is labeled as d. In Fig. 1(a) we notice ϕ is the reflection angle of ϵ, so $\phi = \epsilon$ and $\cos\phi = \cos\epsilon = \frac{s}{d}$. We also notice that $\cos\theta = \frac{\sqrt{d^2-s^2}}{d}$ and $\cos\varphi$ = 1 in Fig. 1(a) and we assume $m = 1$ here. γ_s can be defined as [1] [5]:

$$\gamma_s = \frac{2P_tL_mrA_{tag}A_{PD}g_x^2\beta}{4\pi^2\sigma^2d^2\left(D-\sqrt{d^2-s^2}\right)^2}\left(\frac{s}{d}\right)^2\left(\frac{\sqrt{d^2-s^2}}{d}\right). \tag{4}$$

where L_m is the reflecting power loss after polarized, r is the photo-electronic conversion factor of the PD, β is the reflection coefficient. σ^2 is the noise power.

C. Bit Error Rate

The BER can be used to determine the quality of overall performance in the backscatter communication. The BER is a Q function of SNR (γ_s) for VLC backscattering where Q function is a tail distribution function [13]. So the BER can be given by $P_e = Q\left(\sqrt{\gamma_s}\right) = \frac{1}{\sqrt{2\pi}}\int_{\sqrt{\gamma_s}}^{\infty} e^{\frac{y^2}{2}}\,dy$ [8].

III. Problem Definition

A. Problem Definition for Single Tag Model

Our goal is to find optimal locations of tags to minimize BER. We present a preposition below that shares the key result.

Preposition1 *: Minimization of P_e can be achieved by maximizing γ_s.*

Proof *: The Q function is monotonically decreasing, thus, the minimization of P_e is equivalent to the maximization of γ_s.*

The corresponding optimization problem (P1) is given as:

$$\begin{aligned} &\text{(P1): } \underset{d}{\text{maximize}} \ \gamma_s \\ &\text{subject to} \quad C1: d \le D, \ \ C2: d \ge \delta_0. \end{aligned} \tag{5}$$

Here δ_0 is the minimum distance between any two nodes to be in the radiating far-field region [11].

B. Optimisation Formulation for Two Tags

In the two-tags model, the objective is to maximize the sum of effective SNRs. Since we assume that two tags are working at different times, so we define C as duty cycle which denote the time for which the first tag T_1 is transmitting. Also it needs to noticed that if there are two tags, T_1 is going to block the energy from Tx to T_2, where the block power is donated as P_{block1}. Whereas the T_2 will block the backscattering from T_1 to Rx and, its block power is donated as P_{block2} [16]. These blocking powers are respectively defined below:

$$P_{block1} = A_{tag2}^2\frac{P_t(m+1)^2g_x^2}{16\pi^2d_2^3(D-d_1)^2}\frac{\lambda\Delta_1}{d_1+d_2}. \tag{6}$$

where $\Delta_1 = \cos^m\varphi_2\cos\epsilon_2\cos\phi_2\cos\theta_2$ and A_{tag2} is the cross-section area of T_2.

$$P_{block2} = A_{tag1}^2\frac{P_t(m+1)^2g_x^2}{16\pi^3d_1^2(D-d_2)^2}\frac{\lambda\Delta_0}{d_1+d_2} \tag{7}$$

where $\Delta_0 = \cos^m\varphi_1\cos\epsilon_1\cos\phi_1\cos\theta_1$. λ is the wavelength of the light emitted from Tx. A_{tag1} is the cross-section area of T_1. P_{tag1} below is the energy receiver at T_1 and P_{tag2} is the energy receiver at T_2 [5]:

$$P_{tag1} = \frac{CP_tA_{tag1}g_x^2\,(m+1)\,d_1\cos^m\varphi_1\cos\epsilon_1}{2\pi(D-d_1)^2}. \tag{8}$$

$$P_{tag2} = (1-C)\frac{P_tA_{tag2}g_x^2\,(m+1)\,d_2}{2\pi(D-d_2)^2}\cos^m\varphi_2\cos\epsilon_2. \tag{9}$$

Thus, The sum of effective SNR (γ_{s2}) of two tags model returned as:

$$\gamma_{s2} = \frac{P_{tag1}-P_{block1}+P_{tag2}-P_{block2}}{\sigma^2}. \tag{10}$$

where σ^2 is the noise. Since we objective is to maximize the sum of effective SNR by optimisation of location of tags, the corresponding optimization problem (P2) is given:

$$(P2): \underset{d_1, d_2, C}{\text{maximize}} \quad \gamma_{s2}$$
$$\text{subject to} \quad C3: D \geq d_1 \geq \delta_0, \quad C4: d_2 \geq d_1 + \delta_0, \quad C5: d_2 \leq D, \quad C6: 0 \leq C \leq 1. \tag{11}$$

IV. Optimal location for single tag model

In this section, we will discuss the optimization problem P1. Firstly we will check the convexity of the objective function.

A. Convexity Check

We find second derivative of γ_s to check convexity. As $\frac{\partial^2 \gamma_s}{\partial d^2} = -1.25(ds/D - 0.23)^3$, the $\frac{\partial^2 \gamma_s}{\partial d^2}$ of the objective function in (4) is positive when $ds/D < 0.23$ and is negative when $d > \frac{0.23}{s} D$, so, the function γ_s is concave when $d > \frac{0.23}{s} D$.

B. Optimal location

The SNR defined in (4) is concave when $d > \frac{0.23}{s} D$, we show that only one solution as obtained by solving $\frac{\partial \gamma_s}{\partial d} = 0$ lies on that region. After solving $\frac{\partial \gamma_s}{\partial d} = 0$, we obtain $d = \sqrt{-\frac{1}{3a}(b + \frac{\kappa}{\xi} + \xi)}$, and we notice that there are six solutions according to six different values of ξ. Here $a = 36$, $b = -(96s^2 - 16D^2)$ and $\kappa = 36s^4 - 256D^4 - 4320D^2 s^2$. Those six solutions of γ_s contains three imaginary numbers and only for $\xi = 1, 0.2s^2$ and $152s^2$, the solutions will be real. $d < 0$ when $\xi = 1$. $d > \frac{0.23}{s} D$ when $\xi = 152s^2$ which is optimal value on the range of concave and when $\xi = 0.2s^2$ the solution is convex which is minimum. So we do not consider $\xi = 0.2s^2$ case and the optimal location for single tag is given by:

$$d^* = \sqrt{\frac{56s^2 - 16D^2}{108} + \frac{36s^4 - 256D^4 - 4320D^2 s^2}{152s^2}} \tag{12}$$

Remark 1. *The globally optimal location for single tag is given by d^* in (12) because d^* lies in the concave region, and other feasible roots lie in the convex region. d^* is always larger than δ_0 and smaller than D which satisfies $C1$ and $C2$.*

V. Optimal location for two tags model

In this section, we investigates the optimization problem P2. We start checking the joint convexity of γ_{s2} with respect to d_1, d_2 and duty cycle C. Next, we obtained optimal location of given C follow by optimal C for given locations. Lastly, we find joint optimization in closed-form.

A. Convexity Check

To check the convexity of optimization problem P2, we firstly prove the concavity of γ_{s2} by observing Hessian Matrix and its determinant which are defined below:

$$\nabla^2 \gamma_{s2} = \begin{bmatrix} \sqrt{d_1^3} - d_1^3 & \frac{(D-d_1)-2d_1+1}{(D-d_1)^3} & \frac{1}{(1-C)(d_1+d_2)^2} \\ \frac{(D-d_1)-2d+1}{(D-d_1)^3} & d_1^{\frac{3}{2}} - d_2^{\frac{3}{2}} & 0 \\ \frac{1}{(1-C)(d_1+d_2)^2} & 0 & \frac{d_1-d_2}{(d_2+d_1)^3} \end{bmatrix} \tag{13}$$

$$\det(\nabla^2 \gamma_{s2}) = \frac{(D-d_1)(d_1+2d_1)\sqrt{d_1 d_2}}{(1-C)^2 (d_1-d_2)(D-d_1-d_2)^2} < 0. \tag{14}$$

The determinant of this Hessian Matrix ($\nabla^2\ \gamma_{s2}$) is given by (14) that is negative because $d_1 - d_2 < 0$ under $C4$. Meanwhile, the three principal minors $d_1^{\frac{3}{2}} - d_1^3$, $\frac{d_1-d_2}{(d_2+d_1)^3}$, and $d_1^{\frac{3}{2}} - d_2^{\frac{3}{2}}$ in the 1×1 matrix are all less than zero, and the principal minors of 2×2 matrix, $d_1 d_2 \sqrt{d_1 d_2} + (\frac{(D-d_1)-2d_1+1}{(D-d_1)^3})^2$ and $\frac{(d_1-d_2)(d_1^{\frac{3}{2}} - d_2^{\frac{3}{2}})}{(d_2+d_1)^3}$ are both larger than zero. So the γ_{s2} is jointly concave in d_1, d_2 and C along with the linear constraints $C3$, $C4$, $C5$ and $C6$.

B. Location Optimization

In this section, we find optimal location for a given duty cycle. The objective function is jointly concave so we can find optimal solution by taking derivative for d_1 and d_2 respectively and set them to zero. We start with derivative of d_1. We get four solutions after solving $\frac{\partial \gamma_{s2}}{\partial d_1} = 0$. Under $C3$ of P2, only one solution is feasible.

$$d_1 = \sqrt{\frac{2DC^2(D^2 - 1.35Dd_2 + DCd_2)}{25(D-d_2)^2(1-C)}}. \tag{15}$$

Then, we take derivative for d_2 and have $\frac{\partial \gamma_{s2}}{\partial d_2} = 0$. It is a quadratic functions with two solutions. But one solution is smaller than d_1 which is non-feasible under $C4$, thus, the feasible solution is given below:

$$d_2 = \frac{D(1-C)}{3C} + 0.525 d_1. \tag{16}$$

We substitute (16) into (15) and find the optimal $\widehat{d_1}$ which is given by:

$$\widehat{d_1} = \frac{0.475D + 0.32DC^3 + \sqrt{2.25D^2 + 1.29D + 0.56}}{0.95(1-C)}. \tag{17}$$

Next to find the optimal location $\widehat{d_2}$ we need to substitute (17) into (16) and obtain following result:

$$\widehat{d_2} = \frac{0.5D + 0.3DC^3 + \sqrt{2.25D^2 + 1.3D + 0.56}}{0.6(1-C)} + \frac{D(1-C)}{3C}. \tag{18}$$

C. Duty Cycle Optimization

Here we need to find optimal duty circle C for given locations d_1 and d_2. We need to substitute the d_1 and d_2 into equation (10) so there will obtain an objective function only in term of C and set $\frac{\partial \gamma_{s2}}{\partial C} = 0$. We observe the first derivative of γ_{s2} is a quadratic equation which has two solutions. However, under the constrain $C6$ in P2, one solution of C will be smaller than 1. Thus, the optimal duty cycle for given d_1 and d_2 is given by:

$$\widehat{C} = \frac{24D^2 d_1}{15.38 d_2} + \frac{(1.48 d_2^2 D^2 - 0.7 D^2)^2}{15.38 d_2 \sqrt{2.25D^2 + 1.29D + 0.56}}. \quad (19)$$

D. Joint Optimization

Here we investigate the joint optimization of d_1^*,d_2^* and C^*. To achieve this, we firstly need to substitute optimal $\widehat{C}$ as obtained in (19) into (17) and (18). After substituting $\widehat{C}$, we get two quadratic equations in d_1 and d_2 respectively. On solving d_1 and d_2 respectively, we obtain jointly optimal solution of d_1^* and d_2^* respectively which are shown below which are shown below where satisfy the $C3$, $C4$, and $C5$:

$$d_1^* = \frac{0.3D^2 + D^3 + 0.5D^4 + \sqrt{2.25D^2 + 1.29D + 0.56}}{0.13D + 0.06D^3 + 1.5D^2}. \quad (20)$$

$$d_2^* = d_1^* + \frac{D+7}{D^2 - 7.12D}. \quad (21)$$

In the end, we need to substitute (20) and (21) into (19) to get the joint optimal duty cycle C^* which is shown below:

$$C^* = \frac{\sqrt[3]{(0.56D - 14.12D^2 + 2.28D^3)}\sqrt{D(1.23 + 5.87D)}}{4.5D\sqrt{(2.25D^2 + 1.29D + 0.56)}} + \frac{27.54D}{D^2\sqrt{D} - 4.5D^2}. \quad (22)$$

VI. Numerical Results and Conclusion

The value of D is set as 100m. The areas of square tags and receiver are 0.4m^2.β and L_m are both 0.5. The optoelectronic conversion factor of the PD, r is 0.7 with a fixed noise variance $\sigma^2 = 30$ [5]. The illumination power of each Tx $P_t = 10$W.

A. Single Tag Model

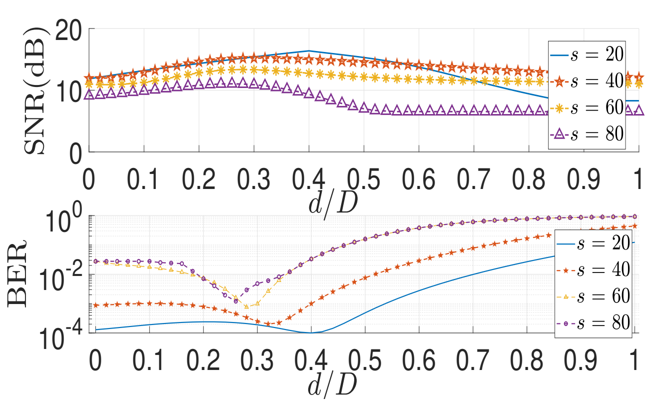

Fig. 2: The relationship of BER and SNR with distance "d"

Fig. 2 above plots SNR and BER as a function of d for different values of s to verify Preposition 1 that maximizing SNR is equivalent to minimizing BER. It indicates that the BER will always be minimized when the tag is closer to the transmitter. It also shows that when s is increased, the location of the tag will be farther from the transmitter so BER increases. The numerical results show that the optimized location of the tag should be closer to the transmitter compared to receiver.

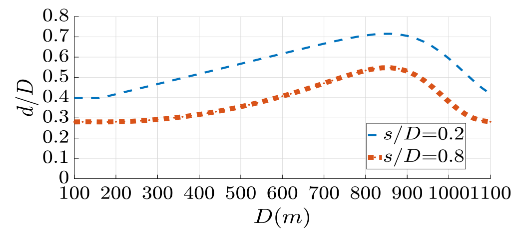

Fig. 3: The optimal d versus different value of D and s

Next we investigate the insights of optimal tag's location on the different s and D. As showing in Fig. 3, the optimal location of tag moves towards to receiver initially but after a certain distant that are 870m it again close to the transmitter.

B. Two Tags Model

In the two tags model we aim to investigate how the effective SNR depends on three variables: d_1, d_2 and C. Specifically, we plot the optimal duty cycle as obtained in

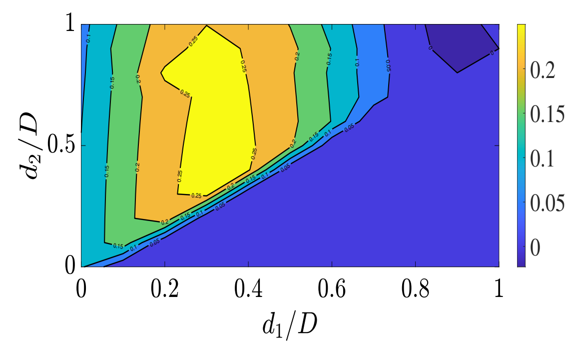

Fig. 4: The optimal C versus different location of tags

(19) as the function of d_1 and d_2 in Fig. 4. It indicates when tags are far away from transmitter T_1 is given less time to work and when tags are near T_1 needs to be given more time. Specifically, when the location of T_1 between the value of $0.2D$ and $0.4D$ it is given most time, otherwise, when T_1 is either very near the transmitter or very far from transmitter, T_2 need to be given more time.

Now we shift to show the relation of maximum effective SNR, optimal $\widehat{d_1}$ and $\widehat{d_2}$ for different value of C and D. In Fig. $5(a)$, $5(b)$ and $5(c)$ we respectively show the maximum effective SNR and optimal location $\widehat{d_1}$, $\widehat{d_2}$ for different values of C and D.

Remark 2. *Two-tags model with low D in Fig. 5, maximum SNR is achieved for $\frac{d_1}{D} = 0.3$, $\frac{d_2}{D} = 0.7$ and $C = 0.25$. SNR*

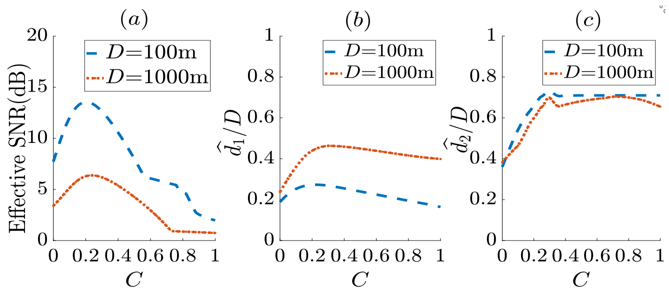

Fig. 5: (a) Effective SNR, (b) optimal location $\widehat{d_1}$, and (c) optimal location $\widehat{d_2}$ for different values of C.

increases when d_1*,* d_2 *and* C *are increasing until* $\frac{d_1}{D} = 0.3$*,* $\frac{d_2}{D} = 0.7$ *and* $C = 0.25$*, then SNR decreases again.*

C. Comparison

Here we come to compare the BER of optimal location for two values of s against three fixed locations which are (1) close to the transmitter, (2) close to the receiver, and (3) at the center. In Fig. 6, the location at the center is better than at the sides and the BER is increasing when s is increasing. The BER at optimal d is 45% lower than it at center when $s = 0.2D$ and 41% lower when $s = 0.8D$.

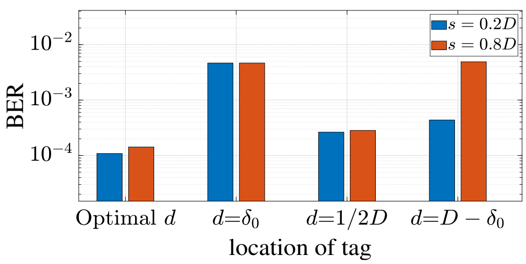

Fig. 6: BER for different values of d in single tag case

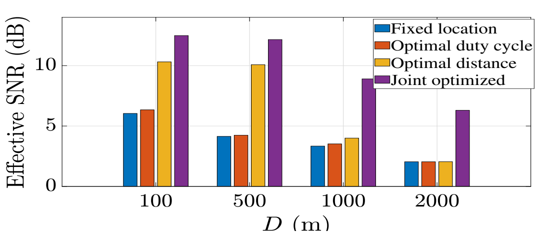

Fig. 7: Comparison of fixed location, optimal duty cycle, optimal location and joint optimization

For the two-tags model, we compare the jointly optimization of location and duty cycle d_1^*, d_2^* and C^* against three fixed allocation schemes on different value of D: (a). fixed $d_1 = 0.5D$, $d_2 = 0.6D$ and $C = 0.5$, (b). optimal $\widehat{C}$, $d_1 = 0.5D$ and $d_2 = 0.6D$, and (c). optimal $\widehat{d_1}$ and $\widehat{d_2}$ while $C = 0.5$. From Fig. 7, the gain improvement by optimal duty cycle, optimal locations and joint optimal schemes over fixed allocation scheme are respectively around 0.6dB, 4.2dB, and 6.4dB when $D = 100$m and around 0.1dB, 5.91dB, and 8.98dB when $D = 500$m. Also the gain improvement by optimal duty cycle, optimal locations and joint optimal schemes over fixed allocation scheme are around 0.22dB, 0.9dB, and 5.56dB when $D = 1000$m. However, when $D = 2000$m there is no significant improvement by optimal duty cycle and optimal locations over fixed location, only the joint optimal scheme improves around 4.26dB over other semi-adaptive schemes. Fig. 7 indicates that the SNR of joint optimization is always better than the semi-adaptive schemes and the SNR decreases when D increases.

References

[1] X. Xu, Y. Shen, J. Yang, C. Xu, G. Shen, G. Chen, and Y. Ni, "PassiveVLC: Enabling practical visible light backscatter communication for battery-free IoT applications," in *Proc. 23rd Annual International Conference on Mobile Computing and Networking*, 2017, pp. 180–192.

[2] "VLC vs RF-difference between VLC and RF communication," https://www.rfwireless-world.com/Terminology/Difference-between-VLC-communication-and-RF-communication.html, 2020, accessed 4 April 2020.

[3] A. Varshney, A. Soleiman, L. Mottola, and T. Voigt, "Battery-free visible light sensing," in *Proc. 4th ACM Workshop on Visible Light Communication Systems*, 2017, pp. 3–8.

[4] J. Wang, "Survey of visible light based backscatter communication, sensing," 2018, http://blizzard.cs.uwaterloo.ca/iss4e/wp-content/uploads/2018/01/Survey-of-Visible-Light.pdf.

[5] X. Wang, K. Han, and M. Zhang, "Modeling the large-scale visible light backscatter communication network," in *Proc. 23rd Asia-Pacific Conference on Communications (APCC)*. IEEE, 2017, pp. 1–6.

[6] D. Mishra and E. G. Larsson, "Multi-tag backscattering to mimo reader: Channel estimation and throughput fairness," *IEEE Transactions on Wireless Communications*, vol. 18, no. 12, pp. 5584–5599, September 2019.

[7] C. Xu, L. Yang, and P. Zhang, "Practical backscatter communication systems for battery-free internet of things: A tutorial and survey of recent research," *IEEE Signal Processing Magazine*, vol. 35, no. 5, pp. 16–27, 2018.

[8] S. Shao, A. Khreishah, and H. Elgala, "Pixelated vlc-backscattering for self-charging indoor iot devices," *IEEE Photonics Technology Letters*, vol. 29, no. 2, pp. 177–180, 2016.

[9] S. M. Navidpour, M. Uysal, and M. Kavehrad, "BER performance of free-space optical transmission with spatial diversity," *IEEE Transactions on Wireless Communications*, vol. 6, no. 8, pp. 2813–2819, 2007.

[10] R. ltd, "Internet of things (IoT) market by software solution (real-time streaming analytics, security solution, data management, remote monitoring, and network bandwidth management), service, platform, application area, and region - global forecast to 2022," https://www.researchandmarkets.com/reports/4308780/internet-of-things-iot-market-by-software, 2020.

[11] D. Mishra and S. De, "Optimal power allocation and relay placement for wireless information and RF power transfer," in *Proc. IEEE international conference on communications (ICC)*. IEEE, 2016, pp. 1–6.

[12] H. Q. Nguyen, J.-H. Choi, T.-G. Kang, S.-K. Lim, D. H. Kim, M. Kang, and C. G. Lee, "Effect of LED emission cross-section in indoor visible light communication systems," *EURASIP Journal on Wireless Communications and Networking*, vol. 2012, no. 1, pp. 1–11, 2012.

[13] T. Komine and M. Nakagawa, "Fundamental analysis for visible-light communication system using LED lights," *IEEE transactions on Consumer Electronics*, vol. 50, no. 1, pp. 100–107, 2004.

[14] S.-H. Lin, C. Liu, X. Bao, and J.-Y. Wang, "Indoor visible light communications: Performance evaluation and optimization," *EURASIP Journal on Wireless Communications and Networking*, vol. 2018, no. 1, p. 228, 2018.

[15] N. Q. Pham, V. P. Rachim, and W.-Y. Chung, "High-accuracy VLC-based indoor positioning system using multi-level modulation," *Optics express*, vol. 27, no. 5, pp. 7568–7584, 2019.

[16] D. Mishra and S. De, "Utility maximization models for two-hop energy relaying in practical RF harvesting networks," in *Proc. IEEE International Conference on Communications Workshops (ICC Workshops)*. IEEE, 2017, pp. 41–46.